GIS-Based Flood Hazard Mapping in Gingoog River, Mindanao

George R. Puno[1], Bryan Allan M. Talisay[2], & Joseph C. Paquit[1]

[1]College of Forestry and Environmental Science, Central Mindanao University, Musuan, Bukidnon, Philippines 8710

[2]CMU LiDAR Project, Musuan, Bukidnon

ABSTRACT

Flooding is one of the most devastating natural disasters in the Philippines, especially in Mindanao. This study aimed to generate datasets of flooding along the Gingoog River based on Geographic Information System (GIS). The method employed simulation and mapping of flood hazards using the Hydrologic Engineering Center's Hydrologic Modeling System (HEC-HMS) and the HEC-River Analysis System (HEC-RAS) within the GIS environment. Rainfall data on December 15, 2015, with a total amount of 20.8 mm and peak discharge of 43.49 m3s-1, were used to simulate flood hazards. The model was calibrated, and its accuracy was tested, and after which, its overall evaluation showed a satisfactory performance, implying applicability to simulate floods during extreme rainfall events. Using Light Detection and Ranging (LiDAR) data, flood maps of the three return periods were generated within HEC-RAS. Results showed that flooding extended up to 2.965 km2, 4.165 km2, and 5.040 km2 with maximum flood depths of 7.77 m, 8.12 m, and 8.49 m for 5-year, 25-year, and 100-year return periods, respectively. The model, together with the hydrologic behavior of the watershed such as the extent of flooding, is very helpful for the development and enhancement of early warning systems in the affected areas.

Keywords: *Flood hazard, GIS, HEC-HMS, simulation*

INTRODUCTION

At the context of the changing climate, the Philippines ranks as the third most hazard-prone countries in the world. Approximately 50.3% of its total area was reported as a natural hotspot, and 81.3% of its population is vulnerable to natural disasters (Senate Economic Planning Office, 2013). One of the most devastating and frequent natural disasters in the Philippines is flooding, which usually hits populated floodplains adjacent to rivers and streams. Adverse effects on the health and safety of localities and the economy of the country are among the major impacts of flooding. With the floodplains' changing nature, there is a need to examine how they are affected by land use change (Abolghasem et al., 2014). In recent decades, Mindanao has been experiencing tropical cyclones with excessive precipitation causing rivers to inundate, sometimes beyond the expectation of the local communities and the local government units. As a consequence, damage to properties and loss of lives due to flooding have become a challenge to the government both at the national and local level.

The Mines and Geosciences Bureau identified Gingoog River in Mindanao to have caused flood hazards in Gingoog City. In 2009, a 1-meter flood affected a total of 2,013 individuals (Gingoog Local Government Unit, 2009). The city's Disaster Risk Reduction Management Council (DRRMC) has seen the need of a flood map with an acceptable level of accuracy to help identify which of the affected areas need to be prioritized during rescue operations. Moreover, a high-precision flood map can lead to a more informed implementation of mitigating measures for efficient and effective disaster risk reduction program of the local government. Precise flooding information is sought for early warning system development in response to the national government's call for a more accurate, integrated, and responsive disaster prevention and mitigation system.

The forecast of river inundation through modeling plays a vital role in the structural and non-structural measures of flood management. The predictions are also useful to prepare the flood maps in floodplain sites using appropriate computer models (Rahman et al., 2011). However, there have been several issues regarding the uncertainty in flood inundation mapping, a probable cause of which can include the techniques used in the process (Merwade et al., 2008). The accuracy and quality of data on ground elevation as well as the geometry of the modeled river have a remarkable impact upon flood mapping (Alho et al., 2009). For several decades, the use of models has been the trend in quantifying flood extents using computer model like the U.S. Army Corps of Engineers Hydrologic Engineering Center's River Analysis System (HEC-RAS). HEC-RAS is an integrated system of software designed for interactive use in a multi-tasking and multi-user network environment. The system is comprised of a graphical user interface (GUI), separate hydraulic analysis components, data storage and management capabilities, and graphics and reporting facilities (USACE, 2002). HEC-RAS provides easy and faster technique of flood mapping with improved precision requirement using available hydrologic data.

The study aimed at creating flood hazard map using HEC-RAS model in the floodplains of Gingoog River in Mindanao, Philippines. Rainfall data on December 15, 2015, with a total amount of 20.8 mm and peak discharge of 43.49 m3s-1 was used to simulate flooding for the 5-year, 25-year, and 100-year return periods. With the integration of LiDAR generated elevation data, the model is expected to provide more accurate flood visualization and forecasting estimates.

The model was calibrated based on the current physical characteristics of the watershed like soils, vegetation, rainfall pattern, and intensity, among others. The accuracy of the model was statistically tested using the Root Mean Square Error (RMSE)-observations standard deviation ratio or RSR, Pearson correlation coefficient (r2), Nash-Sutcliffe Efficiency (NSE), and Percent Bias (PBIAS) criteria. Results show a statistically satisfactory performance with a value of 0.94, 0.92, 0.27, -9.38, for r2, NSE, RSR, and PBIAS estimates, respectively, implying the validity of the model to perform flood simulation during excessive actual precipitation occurrence and for the given return period scenarios. The generated flood map is a valuable tool to enhance the level of preparedness and awareness of the localities and the local government units so that damages to properties and casualties during the disaster are minimized. The information generated by the model is also equally important for a longer term system of risk reduction measures like proper land use zoning, reforestation, and placement of infrastructural control of flood hazards.

METHODOLOGY

Gingoog River is located in the northern part of Mindanao. Its floodplain covers the City of Gingoog, northern coast of the Province of Misamis Oriental. The city is approximately 122 kilometers east of Cagayan de Oro City and 74 kilometers west of Butuan City. It lies on the grid coordinates of 125.1000 E longitude and 8.8167 N latitude. The majority of the watershed's area lies within Gingoog with a small portion falling under the territory of Claveria at the south. Figure 1 shows that Gingoog City is bounded to the east by the Municipality of Magsaysay and Agusan del Norte; to the south by Agusan del Sur, Bukidnon, and part of Municipality of Claveria; to the west by Balingasag and Medina, Misamis Oriental, and to the north by Gingoog Bay.

The watershed of Gingoog has a total land area of 13,383 hectares, 43% of which is within forestland. It has an estimated natural forestland area of 2,550 hectares with closed canopy cover and six (6) waterfalls. The water of this basin drains to Gingoog Bay (Gingoog Local Government Unit, 2009). The basin was purposively chosen in accordance with the priority list for modeling by the University of the Philippines Diliman research team.

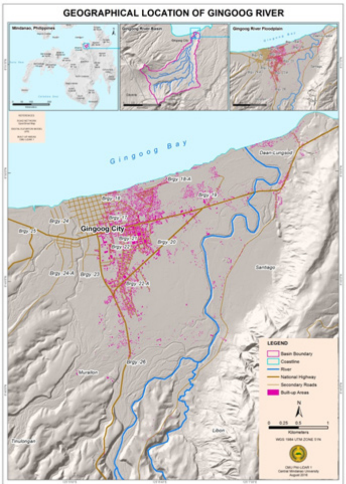

Figure 1. Location map of the study river basin.

Flood modeling at a certain level of accuracy is very challenging. It requires highly skilled researcher, technical protocols, and equipment for data collection, processing, simulation, calibration, and validation. The long and risky method of primary data collection sometimes impedes the field work which may affect data quality requirements (USACE, 2010). Figure 2 summarizes the flow of activities involved in the entire modeling process to generate flood index map for Gingoog River floodplain.

On top of the primary and secondary data collection, the entire modeling process involves preparation of digital elevation model (DEM), setting up and development of HEC-HMS and HEC-RAS models, iterative process of model calibration, and application.

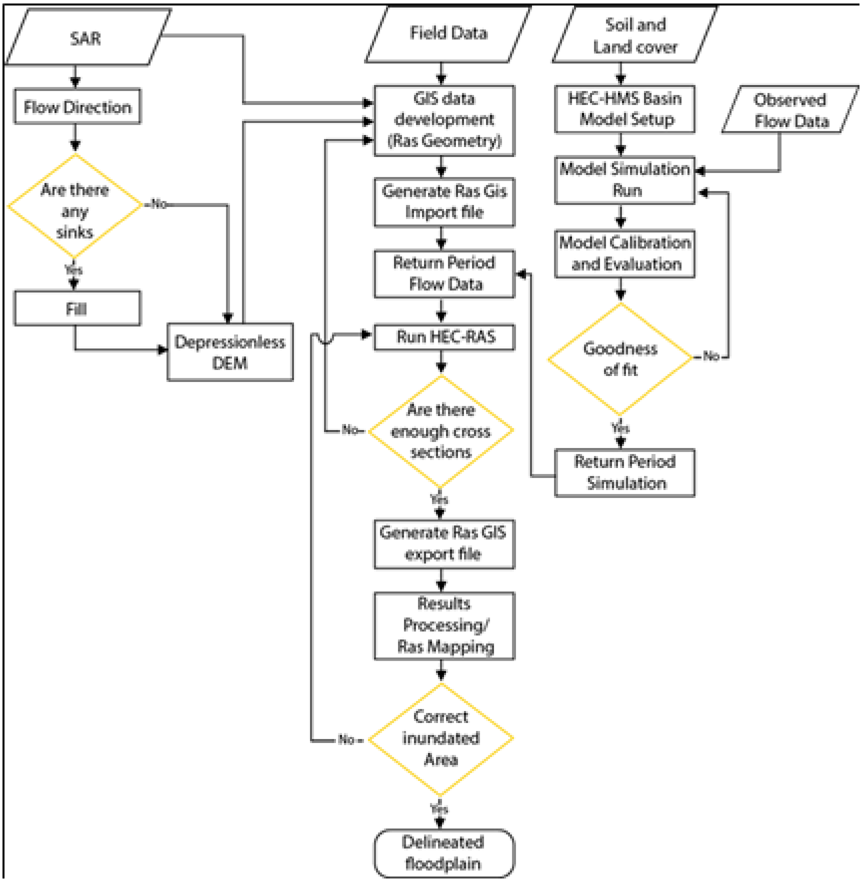

Figure 2. Flow chart of flood simulation and mapping.

The December 15, 2016 event was used in the simulation. Rainfall data at 15-minute interval were collected using automatic rain gauge installed by the Department of Science and Technology–Advanced Science and Technology Institute (DOST-ASTI) at Lurisa National High School, Gingoog City, Misamis Oriental (125.108665 E, 8.763194 N). The rainfall intensity duration frequency (RIDF) values were also obtained from the Philippine Atmospheric Geophysical and Astronomical Services Administration (PAGASA) which were used for the three return period simulations. On the same event, river discharge data were collected at a sampling point beneath the Gingoog hanging bridge using a manual flow meter. The measurement was set to record the velocity of the water as well as the increase of water heights at a 10-minute interval. The rainfall and flow values were used to calibrate HEC-HMS basin model.

The processed and quality-checked data of digital elevation model (DEM) derived from LiDAR point clouds data were obtained. The data were acquired from the University of the Philippines Diliman under the Disaster Risk Exposure and Assessment for Mitigation (DREAM) program, a component of the Nationwide Operational Assessment of Hazards (NOAH) Project of the Department of Science and Technology (DOST). With the river's bathymetric data used to define the morphological features of the riverbed, DEM was used as one of the primary input datasets in the modeling process.

Using HEC-GeoHMS as extension tool of ArcGIS of Environmental Systems Research Institute (ESRI), the basin model of Gingoog River was created (USACE, 2000). HEC-GeoHMS allows users to visualize spatial information, document watershed characteristics, perform spatial analysis, delineates watershed boundaries, and construct inputs to HEC-HMS model. The following datasets were used in model preparation: 10-m resolution Synthetic Aperture Radar–Digital Elevation Model (SAR-DEM) of Gingoog River, main river and stream networks as well as river widths digitized from Google Earth, soil polygon acquired from the Bureau of Soils and Water Management (BSWM) in 2004, and land cover map in 2004 derived from National Mapping and Resource Information Authority (NAMRIA).

The SAR-DEM together with the rivers and stream networks were used to delineate the watershed divide and to produce the reach elements of the model using watershed delineation tools of HEC-GeoHMS. Figure 3 shows the basin model which consisted of 41 sub-watersheds, 20 reaches, and 20 junctions including the main outlet. The delineated sub-watersheds were calculated to have an area ranging from 0.082 to 9.128 km2 with an average of 3.322 km2.

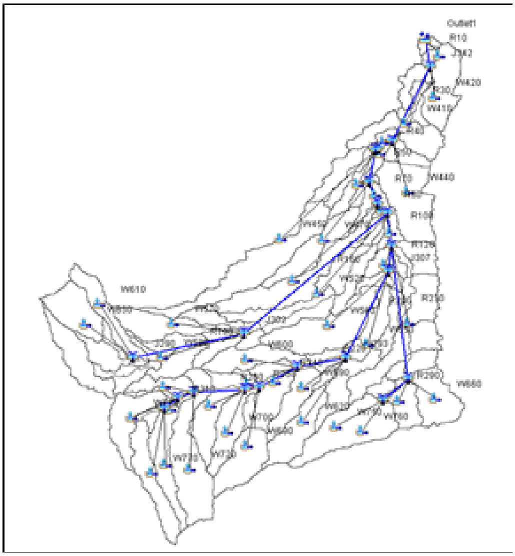

Figure 3. HEC-HMS basin model of Gingoog River.

After several components like the basin and meteorological model, control specification, and time series data were defined and completed in the HEC-HMS interface, the parameters were adjusted based on the prevailing factors such as initial abstraction, curve number, percent impervious, time of concentration, storage coefficient, Manning's n value, among others, considering the movement and response of the hydrograph to provide accurate results of simulated data to the observed data. Manual calibration was done on the HEC-HMS model which provides fast and easy adjustments to a specific parameter. Moreover, the performance of the calibrated discharge was tested using the NSE, RSR, and PBIAS techniques to evaluate the accuracy of the generated model. The NSE is computed as follows:

$$\mathrm{NSE} = 1 - \frac{\sum_{t=1}^{N}[\mathrm{qobs}(t) - \mathrm{qsim}(t)]^2}{\sum_{t=1}^{N}[\mathrm{qobs}(t) - \mathrm{qobs}]^2} \quad \text{Eq. (1)}$$

where qobs (t) is the observed discharge at time step t, qsim (t) is the simulated discharge, qobs is the mean observed discharge over the entire simulation period of length N. The NSE is a normalized measure (–inf to 1.0) that compares the mean square error generated by a particular model simulation to the variance of the target output sequence. An NSE value of 1.0 indicates perfect model performance where the model completely simulates the target output, while a value of 0 indicates that the model is, on average, performing only as good as the use of the mean target value as prediction (Nash & Sutcliffe, 1970).

Moriasi et al. (2007) developed a model evaluation statistic, named the Root Mean Square Error (RMSE)-observations standard deviation ratio (RSR). This technique standardizes RMSE using the observations' standard deviation and is calculated as the ratio of the RMSE and the standard deviation of measured data, as shown in the following equation:

$$\mathrm{RSR} = \frac{\mathrm{RMSE}}{\mathrm{STDEV_{obs}}} = \frac{\sqrt{\sum_{i=1}^{n}(Q_i^{obs} - Q_i^{sim})^2}}{\sqrt{\sum_{i=1}^{n}(Q_i^{obs} - Q_{mean}^{sim})^2}}$$

Eq. (2)

RSR incorporates the benefits of error index statistics and includes a scaling/ normalization factor so that the resulting statistic and reported values can apply to various constituents. RSR varies from the optimal value of 0 to a large positive value and the lower the RSR, the lower the RMSE, and the better the model simulation performance.

Percent bias, on the other hand, measures the average tendency of the simulated values to be larger or smaller than their observed ones. The optimal value of PBIAS is 0.0, with low magnitude values indicating accurate model simulation. Positive values indicate overestimation bias, whereas negative values indicate model underestimation bias (Yapo et al., 1996).

$$\mathrm{PBIAS} = 100\left[\frac{\mathrm{sum(sim-obs)}}{\mathrm{sum(obs)}}\right]$$

Eq. (3)

The calibrated basin model output was then used as the main input file to delineate flood map in the entire process. Using the RIDF data, the same model was used to simulate the discharge values for the predetermined three return periods of 5-, 25-, and 100-years.

Using LiDAR DEM, streamlines were drawn in within the ArcGIS interface to define the paths of the streams. The bank lines were drawn on both sides of the streams to approximate the location of the overbank. Flow lines were also delineated to approximate the flow paths of the center of mass of the main channel, the left overbank, and the right overbank. The flow paths were used to determine the reach lengths between cross sections for the main channel and overbanks or floodplains. Cross sections were created to define the shape of the stream and its characteristics. The layers were then exported to HEC-RAS to run flood simulation.

The file created in HEC-GeoRAS was imported into HEC-RAS through its Geometric Data Editor interface. All the required modification and editing were done at this modeling stage. With a total of 70 cross section lines and an average interval of 200 meters, eight river reaches (total length of approximately 15 km), 16 riverbank lines and four junctions. Some of the cross sections were extended beyond the model domain just to make sure the entire domain is covered. During post-processing, the model results (e.g., flood depth and hazard maps) were clipped accordingly. The resulting geometric representation is shown in Figure 4. Flow resistance coefficients, also called Manning's roughness coefficients n, were assigned to the cross-section segments. The estimated flood discharge derived from the RIDF data of the three return periods of 5-, 25-, and 100-year together with the reach boundary conditions were entered in the interface. The water-surface profiles were then derived from one cross section to the next using the steady module within the HEC-RAS.

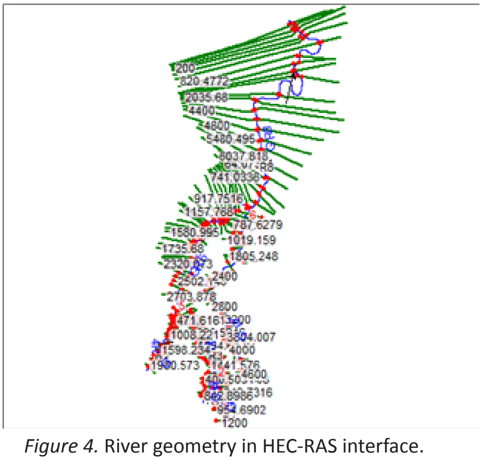

Figure 4. River geometry in HEC-RAS interface.

It involved mapping of the floodplain using the geometric data of the river, terrain and flow data. After the parameters had been prepared, the terrain of the surface was calculated using the interpolation surface tool within the RAS Mapper to delineate flood extents. Figure 5 shows that the water depth grid is created by the subtraction of the rasterized water surface from the terrain data. The 1D output results were viewed within the RAS Mapper after the unsteady flow simulation of the model. The RAS Mapper provides the visualization of the depth layer as well as the flood extent within the study area. The maximum depth and flood boundary of the different return periods were stored in the project directory within the RAS Mapper, and the resulting layers were converted by the program (HEC-RAS) into a float file (FLT file). Then the depth grid layer was imported to ArcGIS and exported to GeoTIFF file (.tif file) for classification of flood hazards and map layout.

Figure 5. Floodplain Mapping using RAS Mapper.

RESULTS AND DISCUSSION

The flood hazards visualization expressed concerning coverage and depth along the floodplain of Gingoog River was simulated with the application of various modeling tools using LiDAR DEM derived from LiDAR point cloud data. Calibration using observed values and fitting of the model based on the existing conditions of the basin were conducted. The performance of the model to forecast flood hazards was examined using standard statistical parameters, and the results are discussed subsequently.

Calibrated Model

Figure 6 shows a comparison of the observed and the simulated discharge data together with the precipitation data from the automatic rain gauge. Total rainfall of 20.8 mm with a peak value of 9.4 mm was recorded on 15 December 2015, at 17:45. The recorded peak discharge was 43.49 m3s-1 during that event.

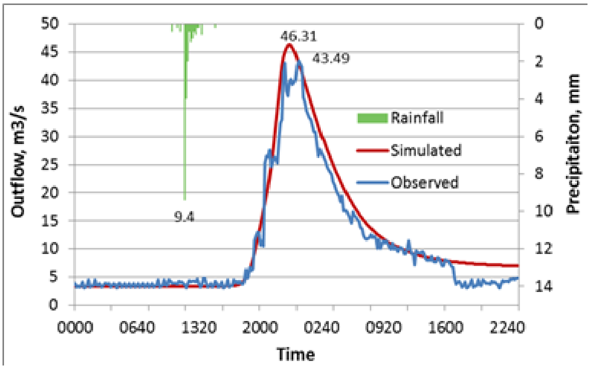

Figure 6. Comparison of observed and simulated discharge with rainfall data.

The calibrated Gingoog HEC-HMS river basin model was tested by comparing it against the observed values using statistical equations (NSE, RSR, and PBIAS) based on the study of Moriasi et al. in 2007 which determine the accuracy of the model shown in Table 1. It was found to have a strong relationship with r2 of 0.94 between observed and simulated values. The model revealed an estimated RSR value of 0.27 indicating higher model's performance to predict values closer to the expected optimum condition completely.

Table 1
General Performance Rating for Model Evaluation

Performance Rating	RSR	NSE	PBIAS
Very Good	0.00 < RSR < 0.50	0.75 < NSE < 1.00	PBIAS < + 10
Good	0.50 < RSR < 0.60	0.65 < NSE < 0.75	+ 10 < PBIAS < + 15
Satisfactory	0.60 < RSR < 0.70	0.50 < NSE < 0.65	+ 15 < PBIAS < + 25
Unsatisfactory	RSR > 0.70	NSE < 0.50	PBIAS > + 25

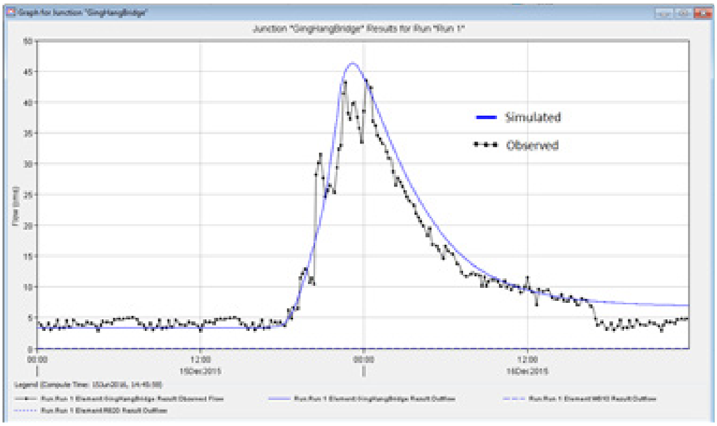

Figure 7. Calibrated discharge of Gingoog River for December 15, 2016, event.

On the same manner, the efficiency of the model was also tested using the NSE technique and revealed a value of 0.92 indicating high predictive power to simulate target outputs. Visual observation shows that there is a very close fit between the observed and simulated flow discharge. Overall, the model met the accuracy test requirements based on the considered statistical parameters implying better predictive performance. However, the PBIAS value of -9.38 indicates that the model has a tendency towards over prediction.

Flood Hazard

Figures also show that the flood provides a discontinuity in some areas. This was due to the abrupt change in elevation which serves as level-high riverbanks or impedance to the inundation of the river. The major road crossing the river located in the northern part (Cagayan de Oro – Butuan highway) has a bridge with high embankment which provides some protection to the local settlers from river flooding. High-water depth occurred along the river channel and extended gradually to the floodplain areas. Results show that the barangays such as Santiago, Daan-Lungsod, including the barangays near the city like Barangays 17 to 26 were also affected. Using the RIDF data, the estimated precipitation for the three return periods of 5-year, 25-year, and 100-year were used to calculate peak discharge values where 478.24 m3, 652.75 m3, and 795.95 m3 were obtained, respectively. These values were subsequently used to simulate flood hazards. The generated flood hazard map shows the flood extent at peak flow for the 5-year, 25-year, and 100-year return periods. The spatial distribution of flood extent is covering in areas with relatively low relief corresponding to agricultural, reclamation, and near river channel which covers an area of about 2.965 km2, 4.165 km2 and 5.040 km2 with maximum flood depths of 7.77 m, 8.12 m, and 8.49 m for the three return periods, respectively. Fosu et al. (2012) conducted a similar study in Susan River – Kumasi using an observed data only with total flooded area covers an approximately 2.93km2 and a flood depth of 4.01637 was obtained.

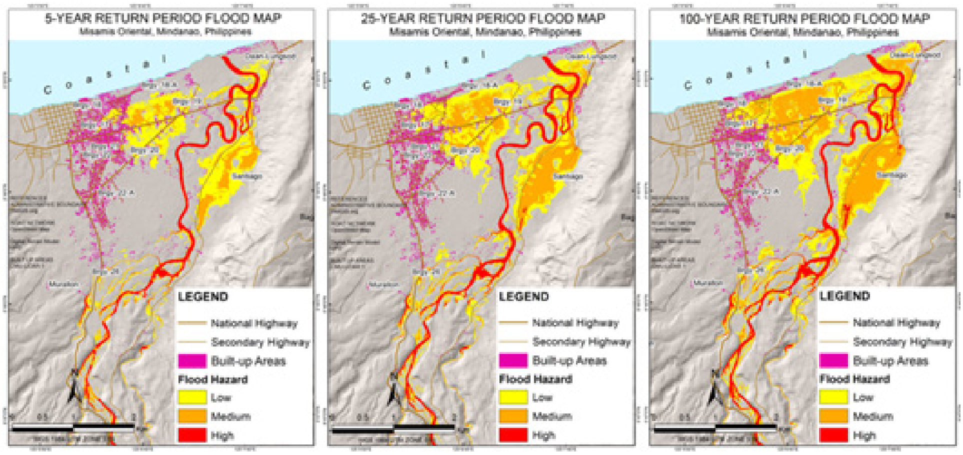

Figure 8. Flood Hazard Map of Gingoog River in 5-year (a), 25-year (b), and 100-year (c) return periods

The result of the overlay identified the affected built-up areas in the barangays of Gingoog City such as residential, commercial, and road network. Based on the UPTCAGP (2013) terminal report, flood hazard was categorized in terms of depths ranges from 0.00-0.5 meter, 0.51-1.50 meters, and > 1.51 meters, indicated with yellow, orange and red in the map were categorized as low, medium, and high, respectively. It was found out during the field reconnaissance that most of the residents in the affected area are informal settlers.

They opted to occupy in areas within sea level for their livelihood which are mostly fishing and small-scale gravel extraction. Observation also showed that portion of the area was previously a reclamation site making it highly vulnerable to flooding.

CONCLUSION

Simulation and mapping of flood hazards along floodplains of Gingoog River were successfully conducted using the combined models of HEC-RAS, HEC-HMS, and ArcGIS of Environmental Systems Research Institute coupled with the use of LiDAR data derived DTM and highly-precise surveying equipment. The model provides vital information to raise the level of awareness and preparedness by the localities and the local government units so that damages to properties and casualties during the disaster are minimized. More specifically, the generated flood hazard index map is a helpful tool for the disaster response unit of Gingoog in their flood monitoring and management, particularly during the rescue and relief goods distribution operations. On the same perspective, the information generated by the model is also equally important for a longer term system of risk reduction measures like proper land use zoning, reforestation, and placement of infrastructural control of flood hazards.

Although the persistently flooded area along the Gingoog River has been simulated and delineated with acceptable results, over-prediction bias as revealed in the estimate of PBIAS cannot be overlooked. Periodic updating and validation of the model are necessary for consistency of model performance considering changes in the modeled environment due to natural and anthropogenic inventions. The lack of intense quality checking in the terrain data for flood mapping also affects the entire outputs of the model. Current high-resolution terrain data derived from LiDAR point clouds with accurately defined river bed integrated with quality bathymetric points are therefore required so that actual terrain models can be created since the accuracy of any hydrological model depends mostly on the quality of the terrain model used.

To account further the validity of the model, individual interview and focus group discussions with the affected residents and local government officials are highly recommended. Affirmative confirmation by the localities is very vital in attesting the reliability and acceptability of the model outputs.

REFERENCES

Abolghasem, A., Golamali, M., Mohsen, F., & Maliheh, S. (2014). Modern Applied Science; Impact of Landuse Change on River Flood plain Using Public Domain Hydrologic Model. *Canadian Center of Science and Education, 8*(5).

Alho, P., Hyyppa, H., & Hyyppa, J. (2009). Consequence of DTM precision for flood hazard mapping: a case study in SW Finland. *Nordic Journal of Surveying and Real Research, 6*(1), 21-39.

Environmental Systems Research Institute (2014). ArcGIS for desktop [Computer software]. Redlands, CA: Environmental Systems Research Institute.

Fosu, C., Forkuo, E. K., & Asare, M. Y. (2012). River inundation and hazard mapping – a case study of Susan River - Kumasi. Department of Geomatic Engineering, Kwame Nkrumah University of Science & Technology, Private Mail Bag, Kumasi, Ghana. Proceedings of Global Geospatial Conference 2012. Québec City, Canada. Retrieved from http://creativecommons.org/licenses/by/3.0/legalcode

Gingoog Local Government Unit. (2009). The Comprehensive Land Use Plan 2010-2019. Gingoog City.

Merwade, V., Olivera, F., Arabi, M., & Edleman, S. (2008). Uncertainty in flood inundation mapping: current issues and future directions. *Journal of Hydrologic Engineering, ASCE.*

Moriasi, D. N., Arnold, J. G., Van Liew, M. W., Bingner, R. L., Harmel, R. D., & Veith, T. L. (2007). Model evaluation guidelines for systematic quantification of accuracy in watershed simulations. Trans. ASABE, 50, 885–900.

Nash, J. E., & Sutcliffe, J. V. (1970). River flow forecasting through conceptual models. Part I: a discussion of principles. *Journal of Hydrology, 10*: 282–290.

Rahman, M., Arya, D., Goel, N., & Dhamy, A. (2011). Design flow and stage computations in the Teesta River, Bangladesh, using frequency analysis and MIKE 11 Modeling. *Journal of Hydrologic Engineering, 16*: 176–186.

Senate Economic Planning Office. (2016, August 15). Natural disaster at a glance. Retrieved from https://www.senate.gov.ph/publications

UPTCAGP. (2013, June). Terminal Report: Surveys and Measurement Technologies for Flood Control, Mitigation and Management Systems: Modeling of Flash flood Events Using Integrated GIS and Hydrological Simulations. University of the Philippines, Diliman, Quezon City.

USACE. (2000). Hydrologic Modeling System HEC-HMS Technical Reference Manual. United States Army Corps of Engineers, Hydrologic Engineering Center, Davis, California. Retrieved from http://www.hec.usace.army.mil/software/

USACE. (2002). HEC-RAS River Analysis System, User's Manual. United States Army Corps of Engineers, Hydrologic Engineering Center, Davis, California. Retrieved from http://www.hec.usace.army.mil/software/

USACE. (2010). HEC-RAS, River Analysis System User's Manual, Version 4.1. United States Army Corps of Engineers, Hydrologic Engineering Center, Davis, California. Retrieved from http://www.hec.usace.army.mil/software/

Yapo, P. O., Gupta, H. V., & Sorooshian, S. (1996). Automatic calibration of conceptual rainfall-runoff models: sensitivity to calibration data. *Journal of Hydrology, 181*: 23-48.